3rd INTERNATIONAL CONGRESS ON ENGINEERING AND LIFE SCIENCE
ICELIS 20-22 SEPTEMBER 2023 TRABZON-TURKIYE

ORAL PRESENTATION https://doi.org/10.61326/icelis.2023.45

Estimating Above-Ground Carbon of Taurus Cedar Stands Using Sentinel-2 Satellite Image: A Case Study of Elmalı Forest Enterprise

***Döndü Demirel*[1]✉, *Alkan Günlü*[2], *Oytun Emre Sakıcı*[1]**

[1]*Kastamonu University, Faculty of Forestry, Kastamonu/TÜRKİYE*

[2]*Çankırı Karatekin University, Faculty of Forestry, Çankırı/TÜRKİYE*

✉***Correspondence***: ddemirel@kastamonu.edu.tr

Abstract: Most terrestrial carbon (C) is stored in forests, an important source of fiber and fuel for humans. Therefore, forests play an essential role in mitigating the effects of climate change by reducing the carbon level in the atmosphere. Field measurements and remote sensing techniques determine the stored above-ground carbon (AGC). This study used Sentinel-2 satellite image to estimate the amount of AGC in pure Taurus cedar (*Cedrus libani* A. Rich.) stands in Elmalı Forest Enterprise. Regression models were developed for AGC estimation with the reflectance and vegetation indices obtained from the Sentinel-2 satellite image. Within the scope of the study, the field measurement data obtained from 120 sample plots were used and AGCs of their corresponding stands were estimated with an allometric equation. The sample plots data was randomly divided into modeling (70%, 84 sample plots) and control data (30%, 36 sample plots) to fit the regression models and to test the accuracy of the models, respectively. Multiple linear regression analysis were conducted to develop the models, and three goodness-of-fit statistics (R^2, *RMSE* and *MAE*) were used to compare the success of these models. When the achievements of the models were evaluated, it was revealed that the model containing the MSR vegetation indice gave more successful results (R^2=0.488). Consequently, it was determined that the developed models were moderately successful in estimating AGC.

Keywords: *Cedrus libani*, AGC, Remote sensing, Vegetation indices, MSR, Sentinel.

1. INTRODUCTION

The Paris Climate Agreement stipulates the reduction of fossil fuel emissions and net neutral carbon emissions by balancing source and sink areas by 2100 (Walsh et al., 2017). At the same time, one of today's most significant issues is reducing greenhouse gas (GHG) emissions by phasing out the infrastructures and technologies that produce fossil carbon emissions (Berndes et al., 2016). Determining the potential of carbon sinks and reducing emissions is crucial (Vashum & Jayakumar, 2012). Oceans, wetlands, rocks and forests are the leading carbon sinks. At the same time, these areas are critical in emission reductions (Dixon et al., 1994; Moomaw et al., 2018). Terrestrial ecosystems are currently a significant net sink for atmospheric CO_2 on a global scale (approximately 1 gigaton C annually) [Canadell & Raupach, 2008].

Forestry is more responsible for a fifth of the world's carbon emissions than the global transport industry. According to Climate Change: Global Forest Financing, a total of $3.7 trillion in long-term savings could be achieved by halving deforestation. However, if nothing is done about deforestation on a global scale, the worldwide economic cost of climate change will be predicted to reach 12 trillion USD (Eliasch, 2008). To monitor and examine climate change, which is directly related to carbon emissions, in temporal and spatial terms, the amounts of carbon released and stored must be determined (Vashum & Jayakumar, 2012).

Traditionally, a forest's above-ground carbon (AGC) stock is obtained through field measurement. This method is expensive, often labor-intensive, time-consuming, and limited area. Instead of traditional methods, remote sensing offers a faster, repeatable, objective and effective way (Myeong et al., 2006). In addition, it allows working in larger areas with less cost and labor. Band reflectance, vegetation indices and various remote sensing data are commonly used to estimate carbon stock with remote sensing (Aricak et al., 2015; Günlü & Ercanlı, 2020; Günlü et al., 2021; Keleş et al., 2021; Turgut & Günlü, 2022; Bulut et al., 2022; Oktian et al., 2022; Sivrikaya & Demirel, 2022).

This study aimed to investigate the possibilities of using Sentinel-2 satellite images in estimating the AGC stock for pure Taurus cedar stands spread in Elmalı Forest Enterprise, Antalya/Türkiye.

2. MATERIALS AND METHODS

2.1. Study Area

The study area includes pure Taurus cedar stands of Elmalı Forest Enterprise, located in the Mediterranean region of Türkiye. This enterprise consists of Çığlıkara, Elmalı and Tekke Planning Units (PU). It is situated between 29°39′00″ and 30°18′00″ Eastern latitudes and 36°27′00″ and 37°00′00″ Northern longitudes (Figure 1). The elevation of the study area varies from 1015 to 3054 m. The study area is 180884.4 ha; approximately 36% (64623.7 ha) of this area consists of forests and 64% (116260.7 ha) of open areas. 42% (26723.8 ha) of the forest area consists of high forests and 58% (37899.9 ha) of degraded forests. The study area has Mediterranean climate. In addition, Brutian pine, Taurus cedar, black pine, Taurus fir, juniper and oak species are common. According to the Köppen climate system, the study area is in the C (temperate) climate group, Csa class, representing the hot summer Mediterranean climate. The C indicates cold, dry and hot summer in the Csa climate type. The coldest month is above 0 °C, the hottest month is above 22 °C, and the average temperature for at least four months is over 10 °C, according to monthly averages. The wettest month of the year experiences at least three times as much rain as the driest month of the year. The driest month of summer sees less than 30 mm of precipitation (Beck et al., 2020).

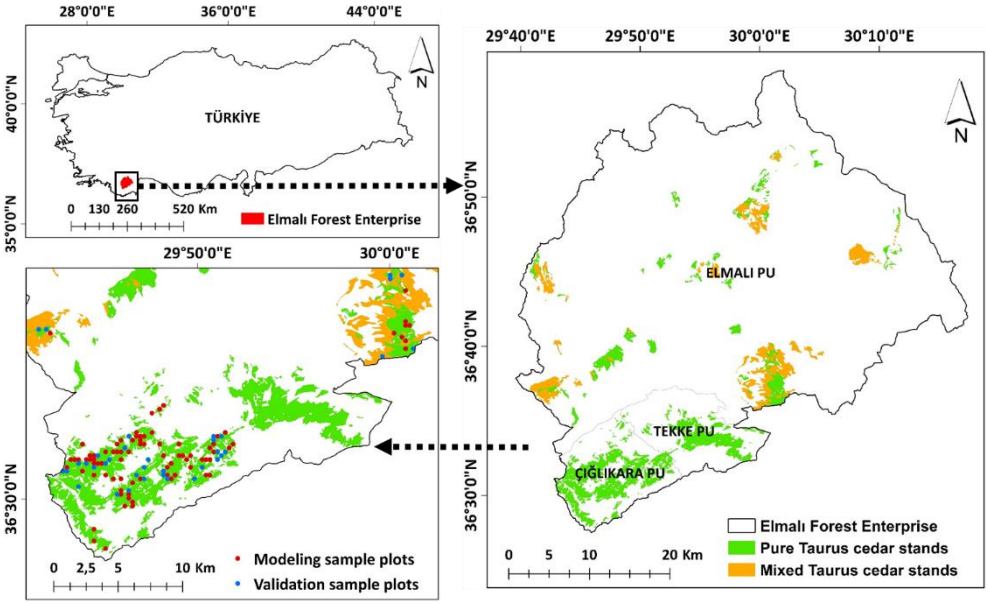

Figure 1. Study area and sample plots**.**

2.2. Field Measurement

In the study, the data obtained from 120 sample plots of pure Taurus cedar stands, taken in 2016 to make the Forest Management Plans of the Planning Units of the Elmalı Forest Enterprise, were used as field measurement data (Anonymous, 2016). Sample plots were taken as circular sample plots of 800 m^2 in stands with 11-40%, 600 m^2 in stands with 41-70%, and 400 m^2 in stands with more than 71% crown closure. The diameter at breast height (*dbh*, cm) of all trees 8 cm and above in each sample plot was measured. The volumes and above-ground carbon amounts of all trees measured in the sample plots were calculated using allometric equations (Equation 1 and 2) developed by Durkaya et al. (2013) for pure Taurus cedar stands in Elmalı region. Then, above-ground carbon stocks of all trees in each sample plot were summed, and stand-level above-ground carbon stocks (t ha^{-1}) were calculated.

$$V = 0.0676 + (-0.0134 * dbh) + (0.001 * dbh^2) \quad (1)$$

$$AGC = 1.518083 + (343.1626 * V) \quad (2)$$

Where; *dbh*, diameter at breast height (m); *V*, stem volume (m^3); *AGC*, above-ground carbon stock (kg).

To create data sets for model development and validation, 120 sample plots were randomly divided into two groups: the modeling data (70%, 84 sample plots) and the validation data (30%, 36 sample plots). Table 1 provides summary statistics of field measurement data.

Table 1. Descriptive statistics of sample plots.

Statistics	Stand volume (m^3 ha^{-1})	AGC (t ha^{-1})
Modeling data (84 sample plots)		
Minimum	18.020	6.639
Maximum	439.560	151.410
Mean	189.991	66.024
Standard deviation	99.850	33.385
Validation data (36 sample plots)		
Minimum	10.393	3.997
Maximum	413.680	142.756
Mean	191.404	66.551
Standard deviation	109.026	37.740

2.3. Remote Sensing Data and Processing

The Sentinel-2 satellite image used in this study was downloaded free of charge from https://dataspace.copernicus.eu. Sentinel-2, starting from 2015, has extended to visible four spectral bands (Bands 2, 3, 4, and 8) at 10 m, near-infrared six bands (5, 6, 7, 8a, 11, and 12) at 20 m and shortwave infrared three bands (1, 9 and 10) at 60 m spatial resolution. Since the field measurements given the data used in the study were obtained in 2016, the Sentinel-2 satellite image dated 24.07.2016 was used to collect remote sensing data. The strip width of this image is 290 km and the temporal resolution is 10 days. Sentinel-2 satellite image was obtained in Level-1 C format, which includes atmospheric, radiometric, and geometric corrections.

The remote sensing data used in this study were reflectance values and vegetation indices. The reflectance was calculated at each sample plot for ten bands (2, 3, 4, 5, 6, 7, 8, 8a, 11 and 12) of the Sentinel-2 satellite image. In order to obtain reflectance values, the satellite image was calibrated using QGIS 3.8.1. To calculate the reflectance values of the sample plots, a "buffer zone" was created according to the sample plot sizes (11.28, 13.82, and 15.96 m radius) using ArcGIS 10.8.1. Reflectance values were obtained by averaging the pixel values within the sample plot boundaries with the "zonal statistics tabulated" command for each band. 32 different vegetation indices obtained from the literature were calculated. The reflectance values of the Sentinel-2 satellite image were used to calculate these indices (Table 2).

Table 2. Calculated vegetation indices.

Vegetation Indice	Reference
BNDVI (Blue-normalized difference vegetation indice)	Yang et al. (2007)
Clgreen (Chlorophyll content)	Gitelson et al. (2003)
Clrededge (Chlorophyll indice rededge)	Gitelson et al. (2003)
CTVI (Corrected transformed vegetation indice)	Perry Jr and Lautenschlager (1984)
CVI (Chlorophyll vegetation indice)	Vincini et al. (2007)
DVI (Differenced vegetation indice)	Richardson and Wiegand (1977)
EVI (Enhanced vegetation indice)	Huete et al. (2002)
EVI2 (Enhanced vegetation indice 2)	Miura et al. (2008)

Table 2. (continued)

Vegetation Indice	Reference
EVI2.2 (Enhanced vegetation indice 2.2)	Jiang et al. (2008)
GARI (Green atmospherically resistant vegetation indice)	Gitelson et al. (1996)
GBNDVI (Green-Blue normalized difference vegetation indice)	Wang et al. (2010)
GEMI (Global environment monitoring indice)	Pinty and Verstraete (1992)
GNDVI (Green normalized difference vegetation indice)	Gitelson et al. (1996)
GLI (Green leaf indice)	Gobron et al. (2000)
GOSAVI (Green optimized soil-adjusted vegetation indice)	Rondeaux at al. (1996)
GRNDVI (Green-Red normalized difference vegetation indice)	Gitelson and Merzlyak (1996)
GSAVI (Green soil adjusted vegetation indice)	Sripada (2005)
GVMI (Global vegetation moisture indice)	Ceccato at al. (2002)
LCI (Leaf chlorophyll indice)	Thenkabail at al. (1999)
MNDVI (Modified normalized difference vegetation indice)	Jurgens (1997)
MSR (Modified simple ratio)	Chen (1996)
NBR (Normalized difference NIR/SWIR normalized burn ratio)	Key and Benson (2005)
NDVI (Normalized difference vegetation indice)	Rouse et al. (1974)
NDWI (Normalized difference water indice)	McFeeters (1996)
NLI (Nonlinear vegetation indice)	Goel and Qin (1994)
PNDVI (Pan normalized difference vegetation indice)	Wang et al. (2007)
PVR (Photosynthetic vigor ratio)	Metternicht (2003)
SAVI (Soil adjusted vegetation indice)	Huete (1988)
SARVI (Soil and atmospherically resistant vegetation indice)	Kaufman and Tanre (1992)
TCARI (Transformed chlorophyll absorption ratio)	Daughtry et al. (2000)
WDVI (Weighted difference indice)	Clevers (1989)
WDRVI (Wide dynamic range vegetation indice)	Gitelson (2004)

As a result, 42 remote sensing data were produced for each sample plot, including 10 reflectance values and 32 vegetation indices using Sentinel-2 satellite image.

2.4. Modeling and Model Validation

Multiple linear regression (MLR) was used to fit the relationships between above-ground carbon (AGC) and remote sensing data (reflectance values and vegetation indices obtained from the Sentinel-2). The stepwise variable selection method was used to generate MLR models for the least squares method. Thus, the success of reflectance and vegetation indice values in AGC prediction was tried to be revealed.

The goodness-of-fit measures used to assess the MLR models included coefficient of determination (R^2), root mean square error (*RMSE*), and mean absolute error (*MAE*).

$$R^2 = 1 - \frac{\sum(y_i - \hat{y}_i)^2}{\sum(y_i - \bar{y})^2} \quad (3)$$

$$RMSE = \sqrt{\frac{\sum(y_i - \hat{y}_i)^2}{n-1}} \quad (4)$$

$$MAE = \frac{\sum|y_i - \hat{y}_i|}{n} \quad (5)$$

These equations use the variables y_i and $\hat{y}_i$ to represent observed and expected AGC, respectively.

The suitability of the models developed to estimate AGC was tested with an independent validation data group. For this purpose, a comparison was made with the Paired Samples *t*-Test using the data obtained from field measurements from the sample plots allocated for validation data and the prediction data calculated for the relevant sample plots with the help of the models developed.

3. RESULTS AND DISCUSSION

The correlation analysis resulted that the DVI, GOSAVI, and GSAVI indices didn't show significant correlation with AGC ($p>0.05$). During the modeling phase, the other reflectance values and vegetation indices were considered as independent variables (Table 3).

Table 3. Correlations between AGC and Sentinl-2 data.

Variable	*r*	Variable	*r*	Variable	*r*
SB4	-0.668**	WDRVI	0.669**	NDWI	0.565**
SB11	-0.634**	GEMI	0.667**	Clrededge	0.477**
SB2	-0.633**	GRNDVI	0.663**	NLI	0.471**
SB12	-0.631**	ChlGreen	-0.649**	SARVI	-0.452**
SB3	-0.598**	GNDVI	0.649**	SAVI	0.427**
SB5	-0.581**	PVR	0.647**	CVI	0.422**
SB8a	-0.461**	GBNDVI	0.639**	EVI	0.378**
SB8	-0.453**	GLI	0.639**	EVI2.2	0.367**
SB6	-0.449**	PNDVI	0.624**	TCARI	0.327**
SB7	-0.434**	BNDVI	0.618**	EVI2	0.294**
GARI	0.672**	LCI	0.604**	WDVI	-0.292**
CTVI	0.669**	GVMI	0.602**	DVI	0.082
MSR	0.669**	MNDVI	0.569**	GOSAVI	-0.069
NDVI	0.669**	NBR	0.569**	GSAVI	-0.076

**Correlation is significant at the 0.01 level. *Correlation is significant at the 0.05 level.

Firstly, the MLR models for AGC were fitted separately for reflectance values and vegetation indices. In the models developed with reflectance values, the coefficient of determination of the model with Band 4 was 0.423, while the model success was 0.456 with the inclusion of Band 6 in the model. The other reflectance values did not make significant contributions. In the models fitted using vegetation indices, the most successful model contained only the MSR indice (R^2=0.488). Then, all remote sensing data (reflectance values and vegetation indices) were tried to fit, but the MSR indice was also an alone independent variable within the final model. As a result, among the developed models, the model with the MSR indice has the highest R^2 and the lowest *RMSE* and *MAE* values (Table 4).

Table 4. Multiple linear regression results for AGC.

Independent variable groups	Independent variables (xi)	Coefficients (bi)	R^2	*SEE*	*RMSE*	*MAE*
Reflectance	Constant	117.107	0.423	25.657	26.673	22.313
	B4	-904.712				
	Constant	73.507	0.456	25.080	25.797	21.511
	B4	-1299.940				
	B6	440.594				
Vegetation Indice	Constant	-17.802	0.488	24.173	24.027	19.926
	MSR	71.593				
Reflectance-Vegetation Indice	Constant	-17.802	0.488	24.173	24.027	19.926
	MSR	71.593				

Paired *t*-test results showed no statistical difference (p>0.05) between the estimated values of AGC and those obtained by field measurements (Table 5). The developed models are suitable for pure Taurus cedar stands from which the data obtained to develop these models.

Table 5. t-test results for models developed for AGC predicted.

Model	Variables	Mean	Standard Deviation	Standard Error of Estimation	*t*	*p*-value
1	B4	70.629	34.318	5.720	-0.712	0.481
2	B4 and B6	72.341	36.358	6.110	-0.948	0.350
3	MSR	70.047	38.289	6.381	-0.548	0.587

According to the residual graphs of the developed models, the estimated AGC values in the model developed with Band 4 show systematic residuals. Similarly, the systematic residual was also observed in the model graph generated with Band 4 and 6. The model developed with MSR, however, shows random residual distribution, in contrast to the models with reflectance values (Figure 2).

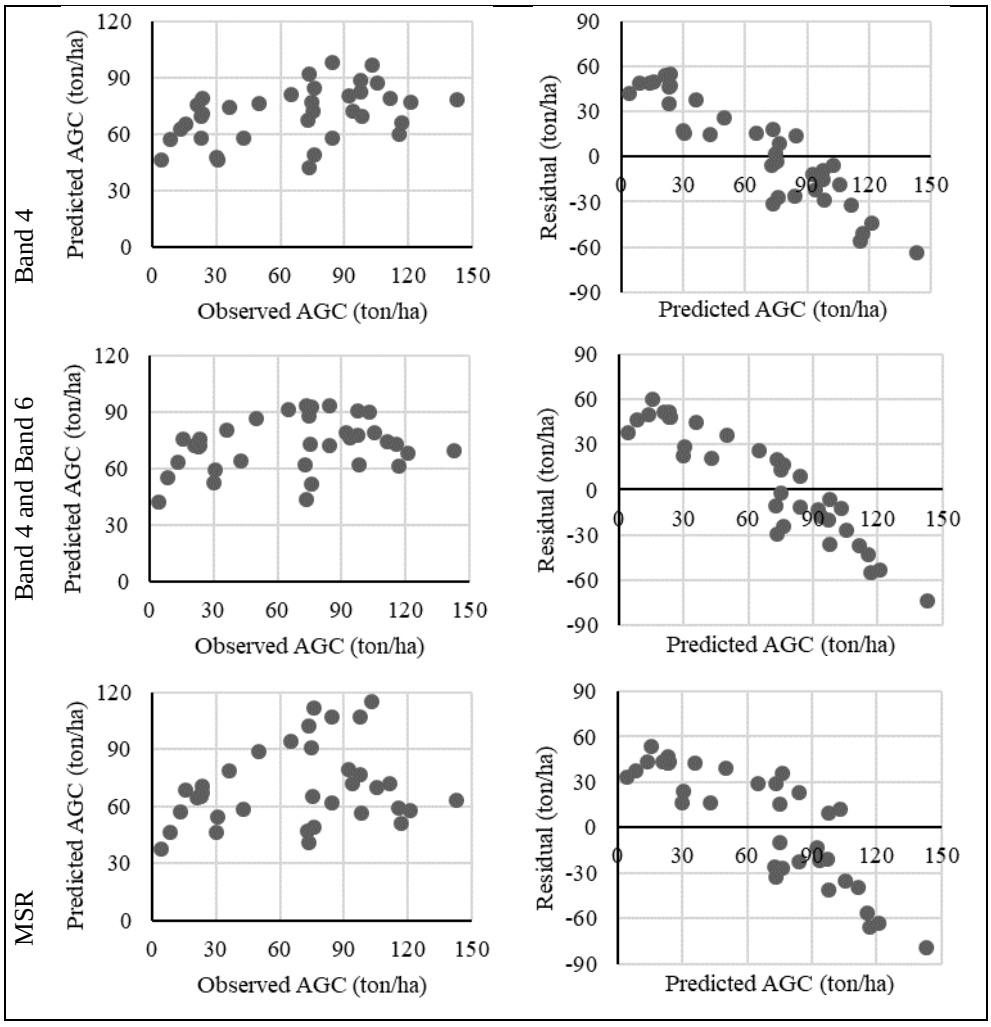

Figure 2. Observed vs. predicted graphs and residual distributions of the models developed.

The best model results for AGC estimations were obtained with independent variable group including the MSR indice (R^2=0.488). On the other hand, model success increased with the inclusion of Band 6 to the reflectance-based models that contained Band 4 (R^2=0.456). In the model with all remote sensing data, i.e., reflectance and vegetation indices were together, the resulting model had the MSR indice only. There are some studies in the literature use Sentinel 2 images and

remote sensing data in modeling the AGC, and this study showed similar results to the literature. Moradi et al. (2022) estimated the AGB in the Hyrcanian forests with the Sentinel-2 satellite image using stepwise regression, and Band 6 gave the most successful model (R^2=0.547). In our study, model success increased also with introducing Band 6 into the model. Nuthammachot et al. (2022) developed the most successful model (R^2=0.820) with NDI45 and Band 6 to estimate AGC with Sentinel-2 satellite image. Keleş et al. (2021) estimated the AGC with the reflectance values using Sentinel-2 satellite image for Hızardere PU in Türkiye. Among the reflectance values, they best predicted AGC with Band 4 (FI=0.454) as in our study. Pandit et al. (2018), in Nepal Parsa National Park, modeled the AGC with 23 different variables (R^2=0.810) using the Random Forest method backward technique with the reflectance and vegetation indices obtained from the Sentinel-2 satellite image. Askar et al. (2018) successfully modeled AGC with the MSR indice (R^2=0.750) using linear regression with Sentinel-2 in Indonesia's Jetis and Girisekar forests. Lu et al. (2022) used the MSR indice from the Sentinel 2 satellite image (R^2=0.580) to estimate the above-ground biomass with regression analysis in the Nan Da Gang Wetland Protected Area in China. Vegetation indices derived from various satellite images have also been researched. In the Bedul Mangrove Block, Purnamasari et al. (2021) predicted the AGC with DVI acquired from PlanetScope image (R^2=0.670). Sivrikaya and Demirel (2022) estimated the AGC in Burmahanyayla PU with Landsat-9. They developed a model to estimate AGC with NDVI obtained from Landsat-9 (R^2=0.623).

4. CONCLUSION

According to the results of this study, R^2 values of the MLR model generated from Sentinel-2 for AGC were found to be 0.488. The best regression result for AGC was obtained with the independent variable group including vegetation indices. The prediction success of AGC models is partially sufficient. The possible reasons for these deficiencies could be the spatial resolution of the satellite image, acquisition time and correction errors, mounting method, topographic and stand structure of the study area, etc. In addition, errors that may occur in measurements during forest inventory affect the model's success. Satellite imagery with high spatial resolution and additional modeling techniques such as machine learning methods (SVM, ANN, RF, K-ENN, etc.) can be employed to improve the performance of regression models in AGC prediction. Sentinel-1 satellite images, which have a higher resolution than Sentinel-2, can be used and received without cost if price is a concern. The use of unmanned aerial vehicle images for remote sensing in forestry, which has lately gained popularity, requires new and updated research.

Acknowledgment

The authors would like to thanks Head of Forest Management and Planning Department, General Directorate of Forestry, Türkiye for their valuable support.

REFERENCES

Anonymous. (2016). *Forest management plans of Elmalı forest enterprise*. General Directorate of Forestry.

Aricak, B., Bulut, A., Altunel, A. O., & Sakici, O. E. (2015). Estimating above-ground carbon biomass using satellite image reflection values: A case study in Camyazi forest directorate, Turkey. *Šumarski List*, *139*(7-8), 369-376.

Askar, A., Nuthammachot, N., Phairuang, W., Wicaksono, P., & Sayektiningsih, T. (2018). Estimating aboveground biomass on private forest using Sentinel-2 imagery. *Journal of Sensors*, *2018*, 1-11. https://doi.org/10.1155/2018/6745629

Beck, H. E., Zimmermann, N. E., McVicar, T. R., Vergopolan, N., Berg, A., & Wood, E. F. (2020). Present and future Köppen-Geiger climate classification maps at 1-km resolution. *Scientific Data*, *7*(1), 1-2. https://doi.org/10.1038/s41597-020-00616-w

Berndes, G., Abt, B., Asikainen, A., Cowie, A., Dale, V., Egnell, G., Lindner, M., Marelli, L., Paré, D., Pingoud, K., & Yeh, S. (2016). *Forest biomass, carbon neutrality and climate change mitigation*. From Science to Policy 3.

Bulut, S., Sivrikaya, F., & Günlü, A. (2022). Evaluating statistical and combine method to predict stand above-ground biomass using remotely sensed data. *Arabian Journal of Geosciences*, *15*(9), 1-14. https://doi.org/10.1007/s12517-022-10140-3

Canadell, J. G., & Raupach, M. R. (2008). Managing forests for climate change mitigation. *Science*, *320*(5882), 1456-1457. https://doi.org/10.1126/science.1155458

Ceccato, P., Gobron, N., Flasse, S., Pinty, B., & Tarantola, S. (2002). Designing a spectral index to estimate vegetation water content from remote sensing data: Part 1: Theoretical approach. *Remote Sensing of Environment*, *82*(2-3), 188-197. https://doi.org/10.1016/S0034-4257(02)00037-8

Chen, J. M. (1996). Evaluation of vegetation indices and a modified simple ratio for boreal applications. *Canadian Journal of Remote Sensing*, *22*(3), 229-242. https://doi.org/10.1080/07038992.1996.10855178

Clevers, J. G. P. W. (1989). Application of a weighted infrared-red vegetation index for estimating leaf area index by correcting for soil moisture. *Remote Sensing of Environment*, *29*(1), 25-37. https://doi.org/10.1016/0034-4257(89)90076-X

Daughtry, C. S., Walthall, C. L., Kim, M. S., De Colstoun, E. B., & McMurtrey III, J. E. (2000). Estimating corn leaf chlorophyll concentration from leaf and canopy reflectance. *Remote sensing of Environment*, *74*(2), 229-239. https://doi.org/10.1016/S0034-4257(00)00113-9

Dixon, R. K., Solomon, A. M., Brown, S., Houghton, R. A., Trexier, M. C., & Wisniewski, J. (1994). Carbon pools and flux of global forest ecosystems. *Science*, *263*(5144), 185-190. https://doi.org/10.1126/science.263.5144.185

Durkaya, B., Durkaya, A., Makineci, E., & Ülküdür, M. (2013). Estimation of above-ground biomass and sequestered carbon of Taurus Cedar (Cedrus libani L.) in Antalya, Turkey. *Iforest-Biogeosciences and Forestry*, *6*(5), 278. https://doi.org/10.3832/ifor0899-006

Eliasch, J. (2008). *Climate change: Financing global forests: The Eliasch review*. Routledge.

Gitelson, A. A., Kaufman, Y. J., & Merzlyak, M. N. (1996). Use of a green channel in remote sensing of global vegetation from EOS-MODIS. *Remote Sensing of Environment*, *58*(3), 289-298. https://doi.org/10.1016/S0034-4257(96)00072-7

Gitelson, A. A., & Merzlyak, M. N. (1996). Signature analysis of leaf reflectance spectra: algorithm development for remote sensing of chlorophyll. *Journal of Plant Physiology*, *148*(3-4), 494-500. https://doi.org/10.1016/S0176-1617(96)80284-7

Gitelson, A. A., Gritz, Y., & Merzlyak, M. N. (2003). Relationships between leaf chlorophyll content and spectral reflectance and algorithms for non-destructive chlorophyll assessment in higher plant leaves. *Journal of Plant Physiology*, *160*(3), 271-282. https://doi.org/10.1078/0176-1617-00887

Gitelson, A. A. (2004). Wide dynamic range vegetation index for remote quantification of biophysical characteristics of vegetation. *Journal of Plant Physiology*, *161*(2), 165-173. https://doi.org/10.1078/0176-1617-01176

Gobron, N., Pinty, B., Verstraete, M. M., & Widlowski, J. L. (2000). Advanced vegetation indices optimized for up-coming sensors: Design, performance, and applications. *IEEE Transactions on Geoscience and Remote Sensing*, *38*(6), 2489-2505. https://doi.org/10.1109/36.885197

Goel, N. S., & Qin, W. (1994). Influences of canopy architecture on relationships between various vegetation indices and LAI and FPAR: A computer simulation. *Remote Sensing Reviews*, *10*(4), 309-347. https://doi.org/10.1080/02757259409532252

Günlü, A., & Ercanlı, İ. (2020). Artificial neural network models by ALOS PALSAR data for aboveground stand carbon predictions of pure beech stands: A case study from northern of Turkey. *Geocarto International*, *35*(1), 17-28. https://doi.org/10.1080/10106049.2018.1499817

Günlü, A., Keleş, S., Ercanli, İ., & Şenyurt, M. (2021). Estimation of aboveground stand carbon using landsat 8 OLI satellite image: A case study from Turkey. In P. Kumar Shit, H. R. Pourghasemi, P. Das & G. S. Bhunia (Eds.), *Spatial modeling in forest resources management: Rural livelihood and sustainable development* (pp. 385-403). Springer. https://doi.org/10.1007/978-3-030-56542-8_16

Huete, A. R. (1988). A soil-adjusted vegetation index (SAVI). *Remote Sensing of Environment*, *25*(3), 295-309. https://doi.org/10.1016/0034-4257(88)90106-X

Huete, A., Didan, K., Miura, T., Rodriguez, E. P., Gao, X., & Ferreira, L. G. (2002). Overview of the radiometric and biophysical performance of the MODIS vegetation indices. *Remote Sensing of Environment*, *83*(1-2), 195-213. https://doi.org/10.1016/S0034-4257(02)00096-2

Jiang, Z., Huete, A. R., Didan, K., & Miura, T. (2008). Development of a two-band enhanced vegetation index without a blue band. *Remote sensing of Environment*, *112*(10), 3833-3845. https://doi.org/10.1016/j.rse.2008.06.006

Jurgens, C. (1997). The modified normalized difference vegetation index (mNDVI) a new index to determine frost damages in agriculture based on Landsat TM data. *International Journal of Remote Sensing*, *18*(17), 3583-3594. https://doi.org/10.1080/014311697216810

Kaufman, Y. J., & Tanre, D. (1992). Atmospherically resistant vegetation index (ARVI) for EOS-MODIS. *IEEE Transactions on Geoscience and Remote Sensing*, *30*(2), 261-270. https://doi.org/10.1109/36.134076

Keleş, S., Günlü, A., & Ercanli, İ. (2021). Estimating aboveground stand carbon by combining Sentinel-1 and Sentinel-2 satellite data: A case study from Turkey. In P. Kumar Shit, H. R. Pourghasemi, P. P. Adhikary, G. S. Bhunia & V. P. Sati (Eds.), *Forest resources resilience and conflicts* (pp. 117-126). Elsevier. https://doi.org/10.1016/B978-0-12-822931-6.00008-3

Key, C. H., & Benson, N. C. (2005). Landscape assessment: ground measure of severity, the composite burn index; and remote sensing of severity, the normalized burn ratio. *FIREMON: Fire effects monitoring and inventory system*, *2004*.

Lu, L., Lu, J., Xin, Y., Duan, H., Sun, Z., Qiu, Y., & Xiao, Q. (2022). How can UAV contribute in satellite-based Phragmites australis aboveground biomass estimating? *International Journal of Applied Earth Observation and Geoinformation*, *114*, 103024. https://doi.org/10.1016/j.jag.2022.103024

McFeeters, S. K. (1996). The use of the Normalized Difference Water Index (NDWI) in the delineation of open water features. *International Journal of Remote Sensing*, *17*(7), 1425-1432. https://doi.org/10.1080/01431169608948714

Metternicht, G. (2003). Vegetation indices derived from high-resolution airborne videography for precision crop management. *International Journal of Remote Sensing*, *24*(14), 2855-2877. https://doi.org/10.1080/01431160210163074

Miura, T., Yoshioka, H., Fujiwara, K., & Yamamoto, H. (2008). Inter-comparison of ASTER and MODIS surface reflectance and vegetation index products for synergistic applications to natural resource monitoring. *Sensors*, *8*(4), 2480-2499. https://doi.org/10.3390/s8042480

Moomaw, W. R., Chmura, G. L., Davies, G. T., Finlayson, C. M., Middleton, B. A., Natali, S. M., Perry, J. E., Roulet, N., & Sutton-Grier, A. E. (2018). Wetlands in a changing climate: Science, policy and management. *Wetlands*, *38*(2), 183-205. https://doi.org/10.1007/s13157-018-1023-8

Moradi, F., Darvishsefat, A. A., Pourrahmati, M. R., Deljouei, A., & Borz, S. A. (2022). Estimating aboveground biomass in dense Hyrcanian forests by the use of Sentinel-2 data. *Forests*, *13*(1), 104. https://doi.org/10.3390/f13010104

Myeong, S., Nowak, D. J., & Duggin, M. J. (2006). A temporal analysis of urban forest carbon storage using remote sensing. *Remote Sensing of Environment*, *101*(2), 277-282. https://doi.org/10.1016/j.rse.2005.12.001

Nuthammachot, N., Askar, A., Stratoulias, D., & Wicaksono, P. (2022). Combined use of Sentinel-1 and Sentinel-2 data for improving above-ground biomass estimation. *Geocarto International*, *37*(2), 366-376. https://doi.org/10.1080/10106049.2020.1726507

Oktian, S. H., Adinugroho, W. C., Anen, N., & Setyaningsih, L. (2022). Aboveground carbon stock estimation model using Sentinel-2A imagery in Mbeliling landscape in Nusa Tenggara Timur, Indonesia. *KnE Life Sciences*, 368-381. https://doi.org/10.18502/kls.v7i3.11145

Pandit, S., Tsuyuki, S., & Dube, T. (2018). Estimating above-ground biomass in sub-tropical buffer zone community forests, Nepal, using Sentinel 2 data. *Remote Sensing*, *10*(4), 601. https://doi.org/10.3390/rs10040601

Perry Jr, C. R., & Lautenschlager, L. F. (1984). Functional equivalence of spectral vegetation indices. *Remote Sensing of Environment*, *14*(1-3), 169-182. https://doi.org/10.1016/0034-4257(84)90013-0

Pinty, B., & Verstraete, M. M. (1992). GEMI: a non-linear index to monitor global vegetation from satellites. *Vegetatio*, *101*(1), 15-20. https://doi.org/10.1007/BF00031911

Purnamasari, E., Kamal, M., & Wicaksono, P. (2021). Comparison of vegetation indices for estimating above-ground mangrove carbon stocks using PlanetScope image. *Regional Studies in Marine Science*, *44*, 101730. https://doi.org/10.1016/j.rsma.2021.101730

Richardson, A. J., & Wiegand, C. L. (1977). Distinguishing vegetation from soil background information. *Photogrammetric Engineering and Remote Sensing*, *43*(12), 1541-1552.

Rondeaux, G., Steven, M., & Baret, F. (1996). Optimization of soil-adjusted vegetation indices. *Remote Sensing of Environment*, *55*(2), 95-107. https://doi.org/10.1016/0034-4257(95)00186-7

Rouse, J. W., Haas, J. R. H., Schell, J. A., & Deering, D. W. (1974). Monitoring vegetation systemsin the Great Plains with ERTS. *In Proceedings of the 3rd ERTS-1 Symposium*, Washington, DC, USA.

Sivrikaya, F., & Demirel, D. (2022). Estimation of aboveground carbon storage based on remote sensing and inventory data: A case study from Türkiye. *Journal of Biometry Studies*, *2*(2), 78-86. https://doi.org/10.29329/JofBS.2022.445.05

Sripada, R. P. (2005). *Determining In-Season Nitrogen Requirements for Corn Using Aerial Color-Infrared Photography*. Pn. D. Dissertation, North Carolina State University, Raleigh, NC, USA.

Thenkabail, P. S., Smith, R. B., & De Pauw, E. (1999). *Hyperspectral Vegetation Indices for Determining Agricultural Crop Characteristics*. New Heawen: Yale University, Center for Earth Observation.

Turgut, R., & Günlü, A. (2022). Estimating aboveground biomass using Landsat 8 OLI satellite image in pure Crimean pine (*Pinus nigra* JF Arnold subsp. *pallasiana* (Lamb.) Holmboe) stands: A case from Turkey. *Geocarto International*, *37*(3), 720-734. https://doi.org/10.1080/10106049.2020.1737971

Vashum, K. T., & Jayakumar, S. (2012). Methods to estimate above-ground biomass and carbon stock in natural forests-a review. *Journal of Ecosystem & Ecography*, *2*(4), 1-7. https://doi.org/10.4172/2157-7625.1000116

Vincini, M., Frazzi, E., D'alessio, P., & Stafford, J. V. (2007). Comparison of narrow-band and broad-band vegetation indexes for canopy chlorophyll density estimation in sugar beet. *6th European Conference on Precision Agriculture*, 3-6 June 2007,189-196, Skiathos, Greece.

Walsh, B., Ciais, P., Janssens, I. A., Penuelas, J., Riahi, K., Rydzak, F., Van, Vuuren, D. P., & Obersteiner, M. (2017). Pathways for balancing CO2 emissions and sinks. *Nature Communications*, *8*(1), 14856. https://doi.org/10.1038/ncomms14856

Wang, F. M., Huang, J. F., Tang, Y. L., & Wang, X. Z. (2007). New vegetation index and its application in estimating leaf area index of rice. *Rice Science*, *14*(3), 195-203. https://doi.org/10.1016/S1672-6308(07)60027-4

Wang, F., Huang, J., & Chen, L. (2010). Development of a vegetation index for estimation of leaf area index based on simulation modeling. *Journal of Plant Nutrition*, *33*(3), 328-338. https://doi.org/10.1080/01904160903470380

Yang, C., Everitt, J. H., & Bradford, J. M. (2007). Airborne hyperspectral imagery and linear spectral unmixing for mapping variation in crop yield. *Precision Agriculture*, *8*(6), 279-296. https://doi.org/10.1007/s11119-007-9045-x